

# Polystyrene–Fluorohectorite Nanocomposites Prepared by Melt Mixing With and Without Latex Precompounding: Structure and Mechanical Properties

S. Siengchin,<sup>1</sup> J. Karger-Kocsis,<sup>1</sup> A. A. Apostolov,<sup>2</sup> R. Thomann<sup>3</sup>

<sup>1</sup>*Institute for Composite Materials, Kaiserslautern University of Technology, Erwin Schrödinger Straße, D-67663 Kaiserslautern, Germany*

<sup>2</sup>*Laboratory on Structure and Properties of Polymers, University of Sofia, BG-1169 Sofia, Bulgaria*

<sup>3</sup>*Institut für Makromolekulare Chemie und Freiburger Materialforschungszentrum, Albert Ludwigs Universität Freiburg, Stefan Meier Straße 31, D-79104 Freiburg, Germany*

Received 15 August 2006; accepted 4 March 2007

DOI 10.1002/app.26474

Published online 19 June 2007 in Wiley InterScience (www.interscience.wiley.com).

**ABSTRACT:** Sodium fluorohectorite (FH) was dispersed in polystyrene (PS) by direct melt blending with and without a master batch composed of PS and FH and produced by latex compounding. FH was not intercalated by PS when it was prepared by direct melt compounding. In contrast, FH was well dispersed (mostly intercalated) in PS via the PS-latex-mediated predispersion of FH following the master-batch route. The dispersion of FH was studied with transmission and scanning electron microscopy and X-ray

diffraction techniques and discussed. The nanocomposites produced by the master-batch technique outperformed the directly melt-compounded microcomposites with respect to stiffness, strength, and ductility according to dynamic mechanical analysis and static tensile tests. © 2007 Wiley Periodicals, Inc. *J Appl Polym Sci* 106: 248–254, 2007

**Key words:** latices; polystyrene; structure-property relationship; thermal properties; WAXS

## INTRODUCTION

The special attention focused on polymer nanocomposites containing various nanoparticles, including layered silicates, is due to their excellent physical-mechanical and promising functional properties.<sup>1,2</sup> Nowadays, the related research is mostly fueled by two aspects: the replacement of organophilic layered silicates by pristine ones and the development of harmless, environmentally friendly production methods. This development is in favor of latex compounding. Many polymers are available in latices after suspension or emulsion polymerization. At the same time, pristine layered silicates swell and thus delaminate (i.e., intercalate) in aqueous media such as latices. Intercalation in water occurs through the hydration of the interstitial cations (usually Na<sup>+</sup>) between the negatively charged silicate layers.<sup>1</sup> Therefore, the production of nanocomposites from a polymer latex and layered silicate is facile and

affordable. However, the latex compounding method has been adopted mostly for rubbers.<sup>3–8</sup> Recently, this method, also termed *heterocoagulation*, was used to produce polyacrylate/clay nanocomposites (the clay was a layered silicate of natural origin).<sup>9,10</sup>

However, polystyrene (PS) is a favored matrix for nanocomposite production with organophilic layered silicates. This is due to the amorphous nature of PS, which allows us to study the intercalation/exfoliation processes in the absence of crystallization. Therefore, Krishnamoorti et al.<sup>11</sup> demonstrated in their early work the effect of polymer diffusion on the intercalation of PS in an organophilic layered silicate. Very recent works on PS/layered silicate nanocomposites dealt with the effects of processing parameters during melt compounding<sup>12</sup> and with the *in situ* polymerization of styrene in the presence of organophilic modified layered silicates.<sup>13–15</sup> The effect of clay particles on film formation from a PS latex was the topic of a recent contribution.<sup>16</sup> The production of water-expandable PS/clay nanocomposite was also solved by the latex route.<sup>17</sup> The promising results for producing nanocomposites via latex compounding with layered silicates led us to study the potential of this approach. Accordingly, this work was aimed at producing PS/sodium fluorohectorite (FH; pristine) nanocomposites through melt-mixing with and without a PS/FH master batch obtained by latex compounding and at comparing

Correspondence to: J. Karger-Kocsis (karger@ivw.uni-kl.de).

Contract grant sponsor: German Science Foundation (through a fellowship to S.S. in the framework of the graduate school); contract grant number: GRK 814.

Contract grant sponsor: Sofia University (to A.A.A.); contract grant number: 126/2006.

*Journal of Applied Polymer Science*, Vol. 106, 248–254 (2007)  
© 2007 Wiley Periodicals, Inc.

the structure–property relationships of the resulting compounds.

## EXPERIMENTAL

### Materials and preparation of the composites

FH (Somasif ME-100, Coop Chemicals, Tokyo, Japan), with an interlayer distance of 0.92 nm and a cation-exchange capacity of 100 mequiv/100 g, served as a filler. PS latex with a 50 wt % dry content (Baystal SX 1160) was supplied by Polymer Latex GmbH (Marl, Germany). This PS latex acted as a swelling and dispersing agent for FH in the master-batch production disclosed later. Granulated PS (Polystyrol 158 K Glasklar, BASF, Ludwigshafen, Germany) was used as polymeric matrix for all composite systems. Its volumetric melt flow rate (melt volume-flow rate at 200°C/5 kg) was 3 cm<sup>3</sup>/10 min.

PS/FH nanocomposites were prepared by two different methods: (1) direct melt compounding and (2) melt compounding using a master batch produced from a PS latex containing FH (master-batch technique). The molecular characteristics of the PSs in the latex and granulate forms were not determined; however, they were similar according to the suppliers' information. The FH content in the corresponding composites was set at 4.5 and 7 wt %, respectively. Melt mixing occurred in a laboratory kneader (type 50, Brabender, Duisburg, Germany) at 180°C and a rotor speed of 60 rpm. The FH powder (direct method) or FH-containing PS master batch (master-batch technique) was introduced after melt mastication (granulates plus dried latex) for 2 min. The duration of the melt mixing for both the direct and master-batch techniques was 6 min.

As the molecular characteristics of the PSs from the latex and granules could be different, attention was paid to set their composition ratios equal in the unfilled and filled composites to be compared. A scheme of the master-batch technique is given in Figure 1. First, an aqueous FH slurry (10 wt %) was produced at the ambient temperature through mechanical stirring for 5 h. Then, the PS latex was introduced into this slurry and stirred for 30 min more. The resulting slurry was poured into a framed glass plate and dried for 48 h at room temperature and for 12 h at 60°C. This condition did not produce a void-free film from the PS latex as the glass-transition temperature ( $T_g$ ) of PS is much higher. However, a void-free film was no prerequisite because of the subsequent melt-mixing process.

The compounds after melt mixing in the Brabender kneader were compression-molded into 1-mm-thick sheets at 200°C with a hot press (EP-Stanzteil, Wallenhorst, Germany).

### Characterization and testing

The dispersion of FH in the PS nanocomposites was studied with transmission electron microscopy (TEM) and X-ray diffraction (XRD). TEM measurements were carried out with a Leo 912 Omega transmission electron microscopic (Zeiss, Oberkochen, Germany) with an acceleration voltage of 120 keV. Thin sections (ca. 50 nm) were cut at room temperature with a diatome diamond knife (Ultracut E microtome, Reichert and Jung, Vienna, Austria). TEM pictures of PS latex particles in the presence and absence of FH were taken after the PS latex was dried on carbon-coated TEM grids at room temperature.

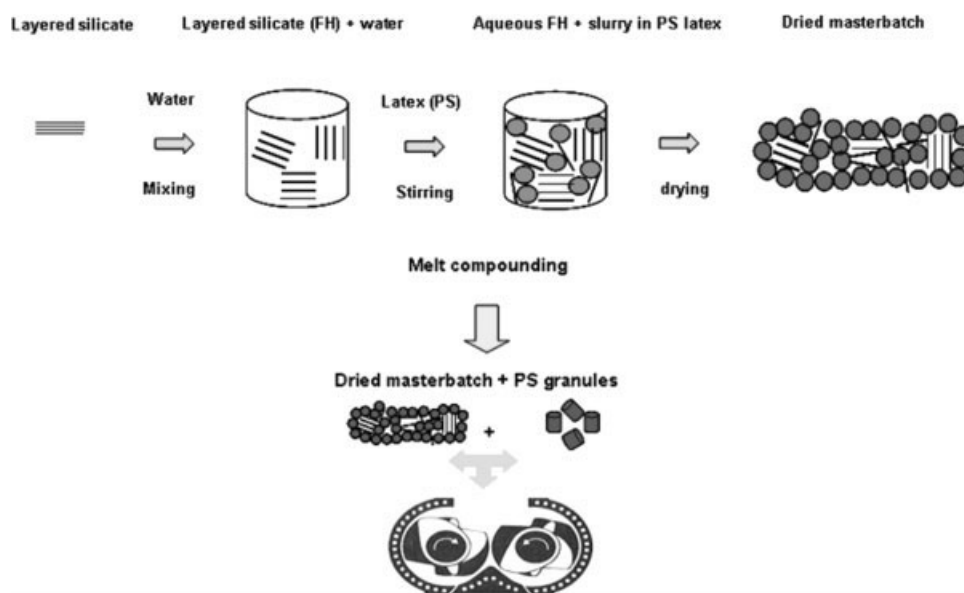
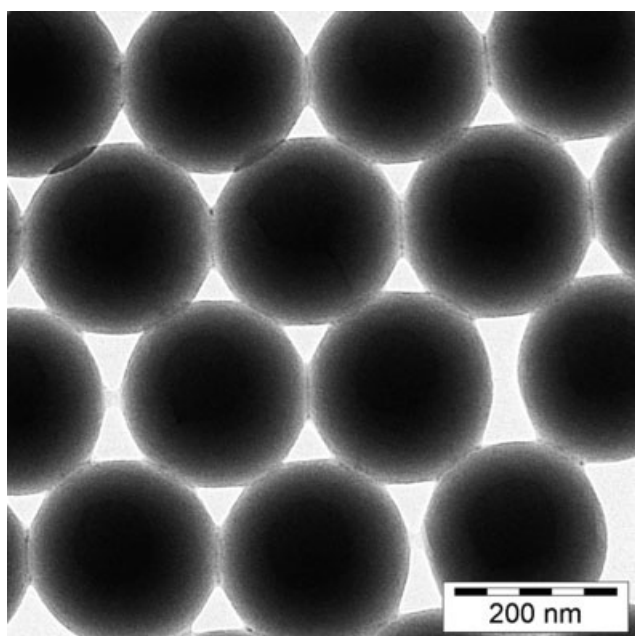
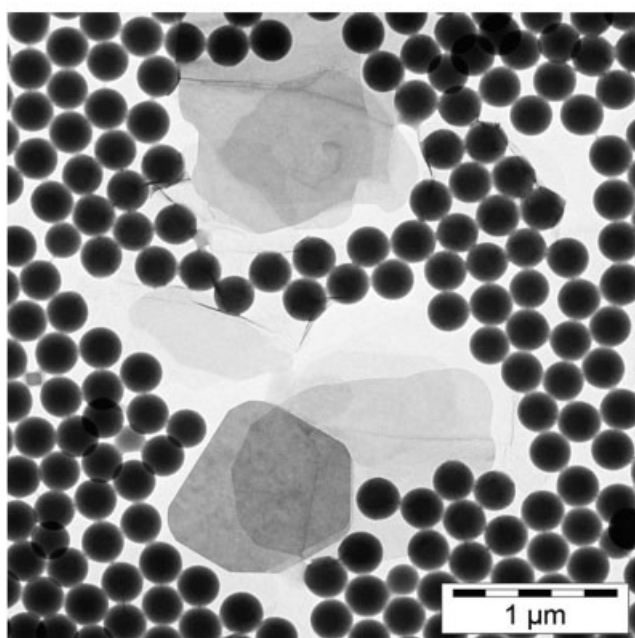


**Figure 1** Scheme of the preparation of PS/FH nanocomposites via the master-batch method.



(a)



(b)

**Figure 2** TEM pictures of (a) a PS latex and (b) a PS latex/FH slurry after the drying of the latex on TEM grids.

XRD spectra in both reflection (FH powder and FH/water slurry) and transmission modes (compression-molded nanocomposite sheets) were collected on a Siemens (Karlsruhe, Germany) D500 diffractometer with Cu K $\alpha$  (40 kV, 30 mA) radiation and a secondary-beam graphite monochromator. The spectra were recorded in the  $2\theta$  range of 1.2–10° in steps of 0.05° and with a counting time per step of 10 s.

To get information about the water swelling of FH, XRD spectra were taken of powder samples containing different amounts of water. The latter was determined gravimetrically after the drying of the samples at 85°C to a constant weight.

Dynamic mechanical analysis was performed in a single cantilever mode at a 1-Hz frequency with a DMA Q800 apparatus (TA Instruments, New Castle, DE). The storage and loss moduli along with the mechanical loss factor were determined as functions of the temperature (–50 to +130°C). The applied strain was 0.01%, and the heating rate was set for 3°C/min. The sample dimensions were 10 × 35 × 3 mm<sup>3</sup> (width × length × thickness).

Tensile tests were performed on dumbbell-shaped specimens (S3A type according to DIN 53504) on a Zwick (Ulm, Germany) 1474 universal testing machine. Tests were run at room temperature and a crosshead speed of 2 mm/min, and the related modulus, strength, and elongation at break values were determined.

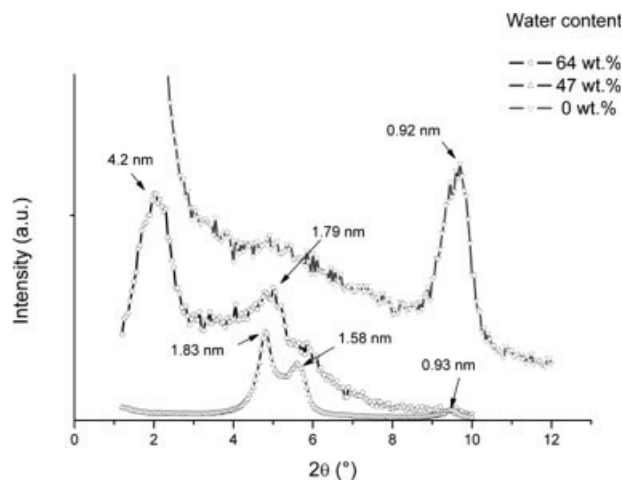
## RESULTS AND DISCUSSION

### Silicate dispersion

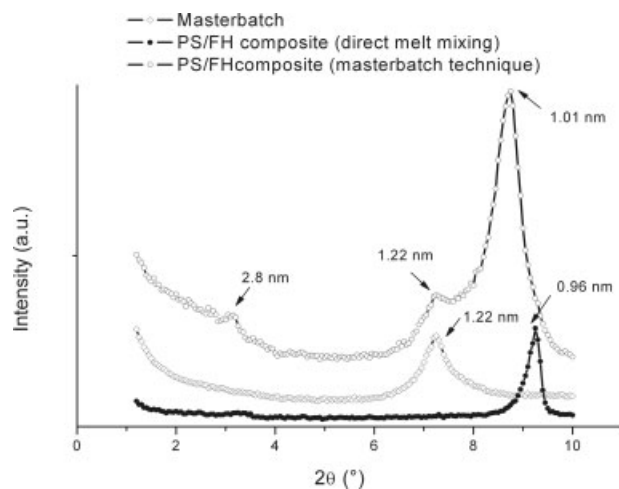
Figure 2 shows that the mean PS particle size is at about 200 nm, and the particles are present in a very narrow distribution. Figure 2(b) informs us about the dimensions of the platy FH. The lateral dimension of the FH platelets may reach 1  $\mu$ m, which corresponds to an aspect ratio greater than 1000. The layer thickness of FH is less than 1 nm.

Figure 2(b) also shows that the FH platelets are likely peeled away from one another, supporting the idea that their intergallery space is swollen in water.

The XRD spectra in Figure 3 evidence, in fact, that water acts as a swelling agent for FH. FH



**Figure 3** XRD spectra of FH as a function of its water content. The spectra were taken in the reflection mode.



**Figure 4** XRD spectra of PS/FH nanocomposites produced by various methods: (●) direct melt mixing (4.5 wt % FH), (○) master-batch technique (4.5 wt % FH), and (◇) master batch from a PS latex/FH slurry (10 wt % FH).

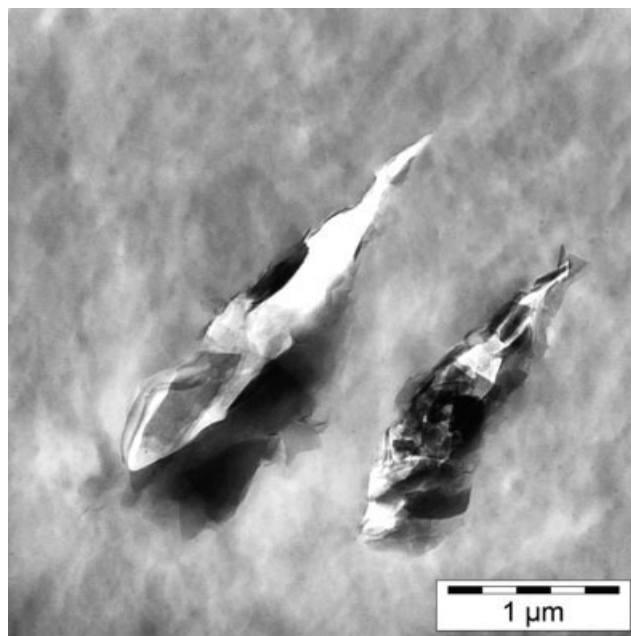
populations with different interlayer distances are present with the same water content. This may be due to several effects (structural inhomogeneity of FH, water diffusion in different FH stacks and agglomerates, and no equilibrium stage), which were, however, not studied in this case.

XRD spectra registered for the differently produced PS composites are shown in Figure 4. One can clearly recognize that direct melt compounding did not result in a nanocomposite, as the change in the intergallery distance ( $d$ -spacing) of FH is negligible (0.96 instead of 0.92 nm). This finding is in agreement with literature results.<sup>18</sup> The compound produced by the master-batch technique has FH populations with different intercalations (2.80, 1.22, and 1.01 nm). Considering the fact that the master batch itself contained intercalated FH ( $d = 1.22$  nm; cf. Fig. 4), one can conclude that during its melt mixing with the PS granule, both further intercalation ( $d = 2.8$  nm) and confinement ( $d = 1.01$  nm) occurred. The latter can be assigned to some reordering of the FH layers during hot pressing. This suggestion is in accord with experimental results achieved mostly on rubbers.<sup>19</sup>

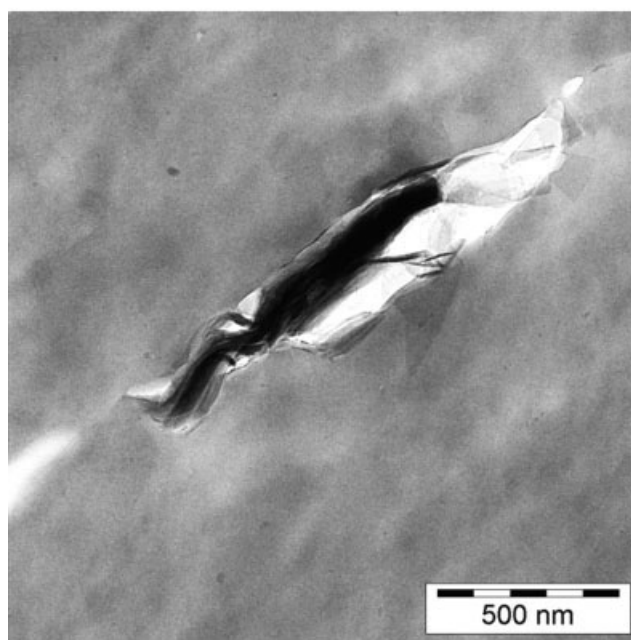
The course of the XRD traces in the low scattering angle range hints at possible FH exfoliation in the master batch and a related PS nanocomposite in contrast to the directly melt-compounded version. The TEM pictures in Figures 5 and 6 corroborate this presumption. The FH stacks are hardly delaminated when the composite (which should correctly be termed a microcomposite) is produced through melt blending (cf. Fig. 5). The FH layers are far better delaminated and dispersed when the nanocomposite is produced by the master-batch method (cf. Fig. 6). Pronounced bending and undulation of the FH

layers suggest that the platelets are well separated (the corresponding stacks are composed of a few silicate layers). The TEM pictures in Figure 6 clearly show that the FH layers are mostly intercalated in the related nanocomposite.

The aforementioned difference in the FH dispersion is well reflected in the dynamic-mechanical and tensile behaviors. Figure 7 depicts the storage modu-

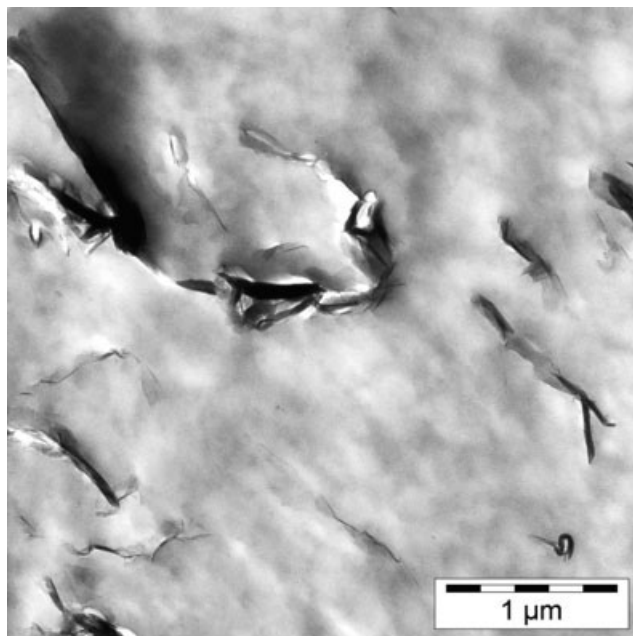


(a)

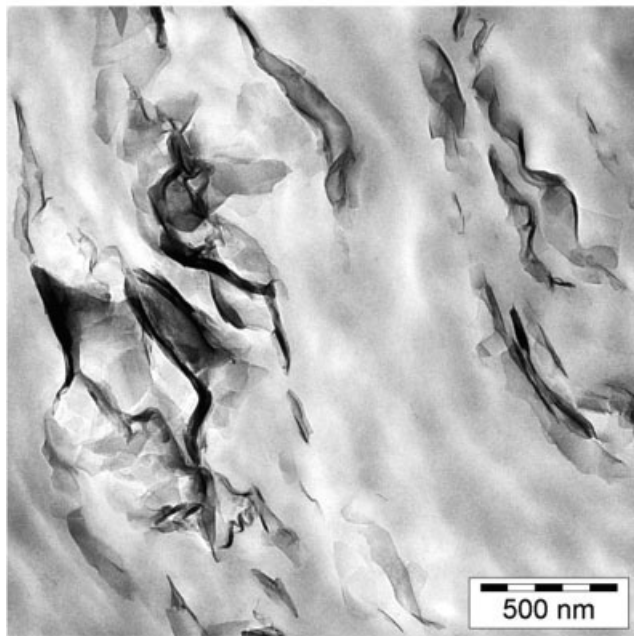


(b)

**Figure 5** Characteristic TEM pictures of a PS microcomposite produced by direct melt compounding. The FH content was 4.5 wt %.



(a)



(b)

**Figure 6** Characteristic TEM pictures of a PS microcomposite produced via the master-batch technique. The FH content was 4.5 wt %.

lus and mechanical loss factor as functions of the temperature for the composites produced by various methods and containing different amounts of FH. The incorporation of FH into PS results in a pronounced stiffness enhancement below the  $T_g$ . This reinforcing effect is accompanied by a shift in the  $T_g$  toward a higher temperature, which is in line with the expectation (the formation of an interphase with

reduced molecular mobility). It is also well resolved that the stiffness of those composites prepared by direct compounding is always inferior to that of those composites produced by the master-batch technique. This can be explained by the consideration of the dispersions of the FH platelets in the related composites, as discussed earlier.

The tensile mechanical data are listed in Table I. The data indicate that an improvement in the stiffness and strength can be achieved at the cost of the ductility (elongation at break). However, the dispersion state of the FH strongly affects the tensile mechanical response. Intercalation and exfoliation of FH enhance the stiffness and strength and reduce the ductility loss of the related nanocomposites at the same time. Large, poorly dispersed FH particles in the melt-mixed microcomposites act as stress concentrations and cause premature failure accompanied by low elongation at break values. The fracture surfaces of the dumbbells show characteristics of brittle fracture. Nevertheless, the difference in the FH dispersion in the composites produced by the methods chosen is obvious in Figure 8. The FH platelets are far better dispersed in PS when prepared via the master batch instead of the direct melt-mixing technique. The well-dispersed FH layers trigger some microductile deformation of the nanocomposite in comparison with the microcomposite, in which the large FH particles induce brittle fracture with voiding [cf. Fig. 8(a,b)]. This is the major reason for the difference in the related ductility values in Table I.

Attention should be paid to the practical relevance of these results. The master-batch technique followed

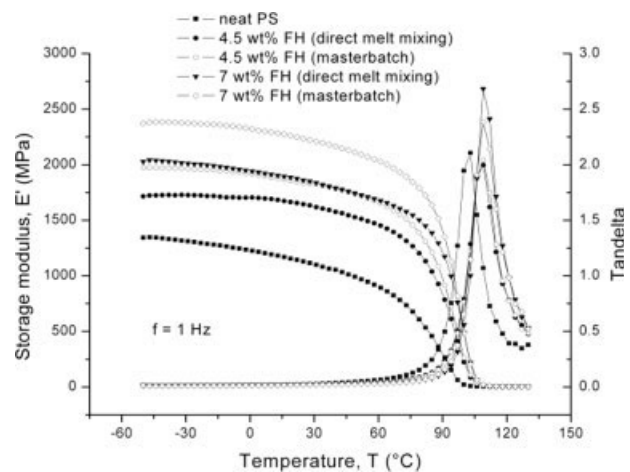


**Figure 7** Traces of the storage modulus ( $E'$ ) versus the temperature and the mechanical loss factor ( $\tan \delta$ ) versus the temperature for PS/FH composites produced by various methods: (■) neat PS, (●) direct melt mixing (4.5 wt % FH), (○) master-batch technique (4.5 wt % FH), (▼) direct melt mixing (7 wt % FH), and (◇) master-batch technique (7 wt % FH).

**TABLE I**  
**Tensile Mechanical Characteristics of the Neat and FH-Reinforced PS Composites Prepared by Various Methods**

Property	Material				
	PS	Master-batch technique		Direct melt mixing	
		PS/4.5 wt % FH	PS/7 wt % FH	PS/4.5 wt % FH	PS/7 wt % FH
Tensile strength (MPa)	25 ± 0.7	39 ± 0.7	41 ± 4	33 ± 1.5	35 ± 5.3
Tensile modulus (MPa)	2917 ± 333	4546 ± 173	5440 ± 258	3667 ± 146	4306 ± 203
Elongation at break (%)	6.3 ± 2.9	1.9 ± 0.4	1.2 ± 0.2	0.8 ± 0.04	0.7 ± 0.06

in this study can be easily performed continuously and online with a well-designed extruder with suitable liquid (latex/slurry) feeding/venting possibilities. It is noteworthy that continuous methods such as the injection of water or a silicate/water slurry have already been suggested<sup>20,21</sup> but never in combi-

nation with latex. The beauty of the simultaneous incorporation of a layered silicate and, for example, a rubber latex is that nanoreinforced and toughened thermoplastics can be produced in this way cost-efficiently.

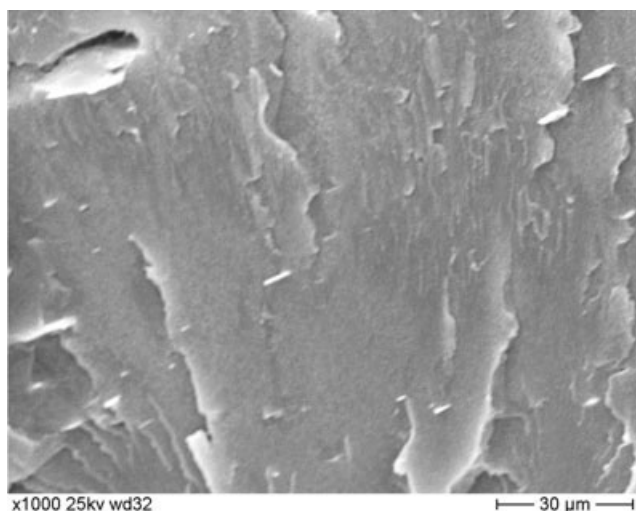
## CONCLUSIONS

On the basis of this work devoted to the study of the potential benefits of PS-latex-mediated dispersions of pristine layered silicates (FH in this case) for the structure and properties of melt-compounded PS nanocomposites, the following conclusions can be drawn:

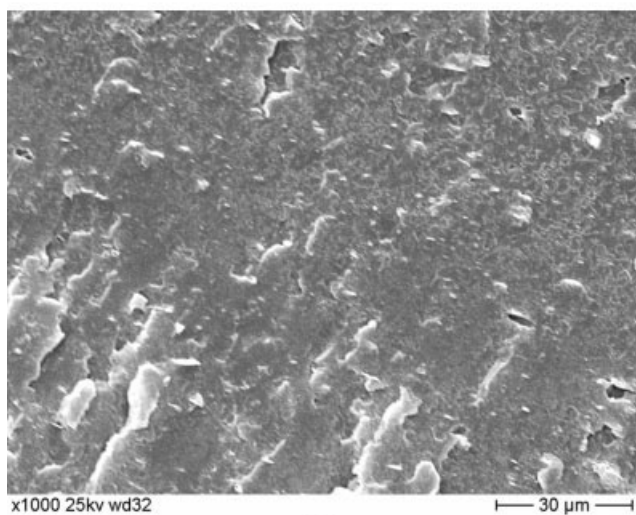
- An intercalated structure is formed when FH is introduced into a PS melt in the form of a master batch. The corresponding master batch is produced through the drying of FH containing a homogenized PS latex. In contrast, the direct introduction of FH into a PS melt (direct melt mixing) results in a microcomposite (limited delamination with hardly any intercalation).
- The stiffness and strength of FH-reinforced PS nanocomposites produced by the master-batch technique are superior to those of composites prepared by melt mixing. The poor dispersion of the FH particles and stacks reduces the ductility of the composites to a larger extent than the good ones characterized by well-delaminated and dispersed FH stacks.

## References

1. Utracki, L. A. *Clay-Containing Polymeric Nanocomposites*; Rapra Technology: Shawbury, UK, 2004; Vols. 1 and 2.
2. Sinha Ray, S.; Okamoto, M. *Prog Polym Sci* 2003, 28, 1539.
3. Varghese, S.; Karger-Kocsis, J. *Polymer* 2003, 44, 4921.
4. Karger-Kocsis, J.; Wu, C.-M. *Polym Eng Sci* 2004, 44, 1083.
5. Wu, Y.-P.; Wang, Y.-Q.; Zhang, H.-F.; Wang, Y.-Z.; Yu, D.-S.; Zhang, L.-Q.; Yang, J. *Compos Sci Technol* 2005, 65, 1195.
6. Valadares, L. F.; Leite, C. A. P.; Galembeck, F. *Polymer* 2006, 47, 672.
7. Varghese, S.; Karger-Kocsis, J. In *Polymer Composites from Nano- to Microscale*; Friedrich, K.; Fakirov, S.; Zhang, Z., Eds.; Springer: Berlin, 2005; p 77.
8. Stephen, R.; Alex, R.; Cherian, T.; Varghese, S.; Joseph, K.; Thomas, S. *J Appl Polym Sci* 2006, 101, 2355.



(a)



(b)

**Figure 8** Scanning electron microscopy pictures of the tensile fracture surfaces of composites produced by (a) the master-batch technique and (b) direct melt compounding.

9. Xu, Y.; Brittain, W. J.; Vaia, R. A.; Price, G. *Polymer* 2006, 47, 4564.
10. Xu, Y.; Brittain, W. J. *J Appl Polym Sci* 2006, 101, 3850.
11. Krishnamoorti, R.; Vaia, R. A.; Giannelis, E. P. *Chem Mater* 1996, 8, 1728.
12. Tanoue, S.; Hasook, A.; Itoh, T.; Yanou, M.; Iemoto, Y.; Unryu, T. *J Appl Polym Sci* 2006, 101, 1165.
13. Yilmazer, U.; Ozden, G. *Polym Compos* 2006, 27, 249.
14. Jeong, H. M.; Choi, J. S.; Ahn, Y. T.; Kwon, K. H. *J Appl Polym Sci* 2006, 99, 2841.
15. Li, H.; Yu, Y.; Yang, Y. *Eur Polym J* 2005, 41, 2016.
16. Uğur, S.; Alemdar, A.; Pekcan, Ö. *Polym Compos* 2006, 27, 299.
17. Shen, J.; Cao, X.; Lee, L. J. *Polymer* 2006, 47, 6303.
18. Giannelis, E. P. *Adv Mater* 1996, 8, 29.
19. Gatos, K. G.; Karger-Kocsis, J. *Polymer* 2005, 46, 3069.
20. Hasegawa, N.; Okamoto, H.; Kato, M.; Usuki, A.; Sato, N. *Polymer* 2003, 44, 2933.
21. Kato, M.; Matsushita, M.; Fukumori, K. *Polym Eng Sci* 2004, 44, 1205.